ORIGINAL

Apoptotic and necrotic basal forebrain cholinergic neuronal loss and dendritic spines alteration after acute and long-term chlorpyrifos exposure: Legal implications of the use of toxicogenomic profile as a biomarker of harmful effects induced under subclinical doses

Muerte de neuronas colinérgicas de la región basal por necrosis y apoptosis, así como alteración de la densidad de espinas dendríticas tras la exposición aguda y a largo plazo a clorpirifos: Implicaciones legales del uso del perfil toxicogenómico como biomarcador de efectos dañinos inducidos a dosis subclínicas

Paula Moyano[1], Javier del Pino[1], María José Anadón[1], José Manuel García[1], María Jesús Díaz[1], Gloria Gómez[1], Jimena García[2], María Teresa Frejo[1] and Miguel Andrés Capó[1]

1. Department of Toxicology and Pharmacology, Veterinary School, Complutense University of Madrid, 28040 Madrid, Spain.
2. Department of Pharmacology, Health Sciences School, Alfonso X University, 28691, Madrid, Spain.

Correspondencia
Javier del Pino PhD
Universidad Complutense de Madrid. Facultad de Veterinaria
Departamento de Toxicología y Farmacología
Avda. Puerta de Hierro s/n 28040 Madrid. Spain
Tel.: 91 355 09 20 – E-mail: jdelpino@pdi.ucm.es

Abstract

Introduction: Chlorpyrifos (CPF) is an organophosphate insecticide reported to induce both after acute and repeated exposure learning and memory dysfunctions, although the mechanism is not completely known. CPF produces basal forebrain cholinergic neuronal loss, involved on learning and memory regulation, which could be the cause of such cognitive disorders. This effect was reported to be mediated through apoptotic process, although neuronal necrosis was also described after CPF exposure. Otherwise, neuronal dendritic spines were reported to be also involved on learning and memory process regulation and their alteration could also contribute to this effect. In this regard, CPF has been reported to induce an alteration in the dendritic spines density in the prefrontal cortex and hippocampus after acute and repeated exposure to subclinical doses respectively, thus their alteration in basal forebrain cholinergic neurons could also mediate cognitive disorders.

Objectives and methods: Accordingly, we hypothesized that CPF induces basal forebrain cholinergic dendritic spine alteration at low concentrations and at higher concentrations produces necrotic and apoptotic cell death. We evaluated in septal SN56 basal forebrain cholinergic neurons, the CPF effect after 24 h and 14 days exposure on dendritic spines, the necrosis induction and the apoptotic and necrotic gene expression pathways.

Results: This study shows that CPF induces after acute and long-term exposure an alteration of dendritic spines at lower concentrations than which induces cell death. Evaluation of cell death pathways and genes related to dendritic spine plasticity revealed that some of them are altered at lower concentrations than which produces the effects observed and below the No Observed Adverse Effect (NOAEL).

Conclusions: The present finding suggest that the use of gene expression profile could be a more sensitive and accurate way to determine the NOAEL.

Keywords: Basal forebrain cholinergic neurons, chlorpyrifos, necrosis, apoptosis, dendritic spines, LOATEL, health legislation

Resumen

Introducción: El clorpirifos (CPF) es un insecticida organofosforado que tras la exposición aguda y repetida, induce disfunciones de los procesos de aprendizaje y memoria, aunque el mecanismo por el cual se produce este efecto no se conoce por completo. El CPF produce en la región cerebral basal anterior la pérdida de neuronas colinérgicas, que participan en la regulación de los procesos de aprendizaje y la memoria, pudiendo ser esta la causa de tales trastornos cognitivos. Se ha observado que este efecto está mediado a través del proceso de apoptosis, aunque también se ha descrito que se produce necrosis neuronal tras la exposición a CPF. Por otra parte, también se ha demostrado que las espinas dendríticas participan en la regulación de los procesos de aprendizaje y memoria y su disrupción también podría contribuir a la alteración de dichos procesos. En este sentido, se ha descrito que el CPF altera la densidad de las espinas dendríticas en la corteza prefrontal y el hipocampo tras la exposición aguda y repetida a dosis subclínicas, respectivamente, por lo que su perturbación en las neuronas colinérgicas de la región basal anterior también podría mediar estos trastornos cognitivos.

Objetivos y métodos: De acuerdo con lo expuesto, nosotros hipotetizamos que el CPF induce, en las neuronas colinérgicas de la región basal anterior, una alteración de las espinas dendríticas a bajas concentraciones y a concentraciones más altas produce muerte celular por apoptosis y necrosis. Evaluamos en neuronas colinérgicas SN56 de la región basal anterior, el efecto del CPF

después de 24 horas y 14 días de exposición sobre las espinas dendríticas, la inducción de necrosis y las vías de expresión génica que median la inducción de apoptosis y necrosis.

Resultados: Este estudio demuestra que el CPF induce, tras la exposición aguda y a largo plazo, una alteración de las espinas dendríticas, a concentraciones más bajas de aquellas a las que induce la muerte celular. La evaluación de las vías de muerte celular y los genes relacionados con la plasticidad de la espina dendrítica reveló que algunos de estos genes están alterados a concentraciones más bajas de aquellas a las que producen muerte celular o alteración de las espinas dendríticas y por debajo del Nivel sin efecto adverso observable (NOAEL) .

Conclusiones: El presente studio sugiere que el uso del perfil de expresión génica podría ser una manera más sensible y precisa para la determinación del NOAEL.

Palabras clave: Neuronas colinérgicas de la region basal anterior basal, clorpirifos, necrosis, apoptosis, espinas dendríticas, LOATEL, regulación sanitaria

Introduction

Chlorpyrifos (CPF) is an organophosphate (OP) insecticide widely used in domestic, agricultural, and industrial applications[1]. Human epidemiological studies have related OPs occupational exposure with neurological and neuro-behavioral deficits including impairments of learning and memory process[2,3]. In this regard, CPF has been shown to produce learning deficits in rats, after acute and repeated administration[4-6]. It has been suggested that inhibition of cholinesterase activity by CPF could be involved in these effects[7]. However, human studies of occupational exposure to OPs often fail to find a significant correlation between blood cholinesterase activity and neuro-behavioral deficits[2,3].

Otherwise, degeneration of septal cholinergic neurons that project to hippocampus has been linked to memory deficits that result from cholinergic modulation of hippocampal synaptic circuit loss[8]. Degeneration of septo-hippocampal cholinergic neurons, as seen in AD and other neurodegenerative diseases, results in loss of cholinergic modulation of septo-hippocampal synaptic circuits that leads to memory deficits[8]. In fact, the severity of memory deficit is strongly correlated with the degree of cholinergic cell loss[9]. Thus, cholinergic neuronal loss in this region could be related with CPF impairment of memory function among other actions[10].

In this regard, Lopez-Granero et al[4] reported that chronic dietary exposure in rats produced cognitive and emotional disorders related with changes in AChE forms. In addition, Del Pino et al[11] reported that CPF induced, after acute and long-term exposure, apoptotic cell death in cholinergic neurons from the basal forebrain and this effect was independent of AChE inhibition and acetylcholine level alteration, but was mediated partially by AChE-R and AChE-S overexpression, supporting the idea that the cognitive disorders reported after CPF exposures may be produced by induction of basal forebrain cholinergic cell loss mediated partially through AChE forms alteration. In addition, CPF has also been reported to induce neuronal cell death through necrosis process after CPF acute and long-term exposure[12,13], thus the cell death observed could be also mediated through necrosis induction by CPF. In this regard, previously Del Pino et al[14] reported that AChE-R and AChE-S overexpression induces at low concentrations apoptosis and necrosis at high concentrations in basal forebrain cholinergic neurons, supporting our hypothesis.

Otherwise, loss of dendritic spines has been reported in neurodegenerative disorders as AD affecting mostly selective neuronal networks of critical importance for memory and cognition, such as the basal forebrain cholinergic system, the medial temporal regions, the hippocampus and many neocortical association areas[15] inducing cognitive disorders[16,17]. In this regard, CPF has been reported to induce an alteration in the dendritic spines density in the prefrontal cortex and hippocampus after acute and repeated exposure to subclinical doses respectively[18,19]. Moreover, cognitive disorder has been reported to be produce from subclinical doses and from a lower doses from which basal forebrain cholinergic cell loss has been reported[20], as happens with dendritic spines alteration.

According to these data, we hypothesized that CPF induces basal forebrain cholinergic dendritic spine alteration at low concentrations and at higher concentrations produces neuronal loss through necrosis and apoptosis. The present work intends to study the CPF mechanisms of basal forebrain cholinergic neuronal loss and dendritic spine alteration, due to the importance of these effects to explain CPF toxicity on cognitive disorders and neurodegenerative diseases symptoms like. To reach this aim we treated with CPF for 24 h or repeatedly for 14 days, wild type or transfected with siRNA for AChE, SN56 cells from basal forebrain as an *in vitro* model of cholinergic neuronal cells from this region to research the CPF effect on dendritic spines and expression of genes involved in dendritic outgrowth, the necrotic cell death induction through AChE splice variants alteration and the apoptotic and necrotic gene expression pathways related to cell death process.

Materials and methods

Chemicals

The compounds chlorpyrifos (99.99%), poly-L-lysine, dibutyryl-cAMP, retinoic acid, 3,3´-diaminobenzidinetetrachloride, anti-microtubule-associated protein-2 (MAP-2) monoclonal antibody and paraformaldehyde were obtai-

ned from Sigma (Madrid, Spain). All other chemicals were reagent grade of the highest laboratory purity available.

Culture of SN56 cells

SN56 cells, a cholinergic murine neuroblastoma cell line derived from septal neurons[21], were used as a model of cholinergic neurons from basal forebrain to evaluate CPF toxic effects on this specific type of neurons and the mechanisms through which they are induced. The cells were maintained at 37ºC and 5% CO_2 in Dulbecco's Modified Eagle's Medium (DMEM) supplemented with 10% fetal bovine serum (FBS), penicillin/streptomycin, 2 mM L-glutamine (Sigma, Madrid, Spain), and 1 mM sodium pyruvate. Medium was changed every 48 h[22]. Differentiation of the cells was achieved by culturing for 3 days with 1 mM dibutyryl-cAMP and 1 µM retinoic acid as described[23,24], which produce morphological maturation and 3-4-fold increase of ChAT activity and acetylcholine level in the cells. Differentiated cells have been reported to be more sensitive to neurotoxic compound that affects cholinergic pathways[23,24].

In order to determine the dendritic spine density, the cellular lactate dehydrogenate (LDH) content in wild type and siRNA AChE transfected cells, the apoptotic and necrotic main gene expression pathways, and the expression of the main genes related with dendritic spines plasticity, cells were seeded in 6-well plates at a density of 10^6 cells/well. Cells were treated for 24 h or for 14 days with CPF in concentrations between 0.01 µM to 70 µM and 0.01 µM to 40 µM respectively. At least 3 replicate wells/treatment were used. A vehicle group was employed in parallel for each experiment as a control.

In the literature, 10–100 µM chlorpyrifos has been routinely used to study chlorpyrifos toxicity[25-28], although there are not enough data regarding the relative distribution or concentration of CPF in human brain after acute and chronic exposure. In addition, studies have shown that the blood plasma concentration of CPF from human volunteers were similar to 0.1 µM[29]. Moreover, whole-body molar concentrations associated with the doses of CPF (2.5–25.0 mg/kg/day) used in behavioral experiments have been reported to be calculated as ranging between approximately 7.0 and 8.0 to 70.0 and 80.0 µM[20]. The NOAEL set for CPF is 0.1 mg/kg bw per day[30], which would be around 0.3 µM concentration in the tissues according to Terry et al[20]. The used doses appear to be relevant to study the cognitive disorders according to all described above. Furthermore, we chose CPF 30 µM concentration, which was the lowest concentration observed to induce cell death after acute exposure[11], to study the CPF necrotic and apoptotic mechanisms.

Lactate dehydrogenase (LDH) assay

The necrotic cell death was assessed by measuring the LDH released into the culture medium using Lactate Dehydrogenase Activity Assay Kit (Sigma-Aldrich, Madrid, Spain) according to the manufacturer's instructions. Briefly, the culture medium was removed and pipetted into 96-well plates. The Master Mix reagent was added, and after 3 min colorimetric intensity was determined at 450 nm over every 5 min using a microplate spectrophotometer (Fluoroskan Ascent FL Microplate Fluorometer and Luminometer, ThermoFisher Scientific, Madrid, Spain).

Gene knockdown

SN56 cells were transfected with siRNAs in 6-well plates (1 x10^6 cells/well) using HiPerfect Transfection reagent according to the manufacturer's instructions (Qiagen, Barcelona, Spain). Two sets of siRNA duplexes (Qiagen, Barcelona, Spain) homologous to mouse AChE sequence were designed using the Hi-Performance Design Algorithm (Norvatis AG) and were purchased from Qiagen (catalog numbers GS11423 a). As a transfection control, an All Stars Negative Control siRNA (Qiagen, Barcelona, Spain) was used. 48 h after transfection, the efficiency of siRNA-mediated AChE was determined by RT-PCR using primers specific for mouse AChE mRNA (Qiagen, Barcelona, Spain). The effects of AChE knockdown on cell injury were tested by LDH cell viability assay. After 24 h of incubation with the siRNAs, the cells were washed with PBS and incubated for a further 24 h or 14 days in culture medium with or without CPF.

Protein determination

At the end of the treatments, SN56 cells were washed with pre-chilled PBS, collected by scrapping, and lysed using RIPA buffer (Thermo Scientific, Madrid, Spain) with freshly added protease inhibitors cocktail (ThermoFisher Scientific, Madrid, Spain). After centrifugation at 10,000 x g for 10 min at 4ºC, cell lysate supernatant was collected. Protein concentration was assayed using a BCA kit (ThermoFisher Scientific, Madrid, Spain) and normalized.

Dendritic spines density determination.

SN56 differentiated cell were suspended in DEMEM medium. Cells suspension was plated at a density of 106 cell/ml onto poly-L-lysine 0.10 mg/mL coated glass coverslips (22 mm diameter) placed in plastic Petri dishes (35 mm diameter) coated with poly-L-lysine. Coverslips with adhered SN56 cells were fixed with ice-cold 4% (w/v) paraformaldehyde for 15 min and then placed into 0.5 M potassium/PBS (KPBS) until use. Coverslips were washed three times in KPBS, and cells were permeabilized with 50% ethanol for 1 h and blocked with 10% normal goat serum in 0.1% Triton X-100-supplemented KPBS (0.1% KPBST). After three 15 min KPBS washes, coverslipped cells were then incubated overnight in primary anti-microtubule-associated protein-2 (MAP-2) monoclonal antibody at 1:1000 dilution in 0.1% KPBST at 4°C. Three washes of 0.1% KPBST was then followed by immersion for 2 h in secondary anti-mouse antibody conjugated to biotin (Vector Laboratories) diluted 1:500 in 0.1% KPBST, washed in 0.1% KPBST, and visualized using Vectastainavidin–biotin horseradish peroxidase complex (Vector

Laboratories, Barcelona, Spain) at 1:1000 dilution in 0.1% KPBST for 1 h before staining with 0.05% (w/v) 3,3′-diaminobenzidinetetrachloride, 0.005% (v/v) H_2O_2, and 2.5% (w/v) nickel (II)sulfate in 0.175 M sodium acetate[31]. MAP-2 protein is not localized in dendritic spines but allows for accurate quantification of dendritic spine density.

Real-time PCR analysis

Total RNA was extracted using the Trizol Reagent method (Invitrogen, Madrid, Spain). The final RNA concentration was determined using a spectrophotometer Nanodrop 2000 (ThermoFisher Scientific, Madrid, Spain) and the quality of total RNA samples was assessed using an ExperionLabChip (Bio-Rad, Madrid, Spain) gel. First-strand cDNA was synthesized with 1000 ng of cRNA by using a PCR array first strand-synthesis kit (C-02; SuperArray-Bioscience, Madrid, Spain) following the manufacturer's instructions and including a genomic DNA elimination step and external RNA controls. After reverse transcription, we performed QPCR using the mouse Cell Death PathwayFinder PCR Array (PAMM-212Z) used to analyze mRNA levels of 84 key genes involved in cell death, in a 96-well format, according to the manufacturer's instructions (SABiosciencesInc). Reactions were run on a CFX96 using Real-Time SYBR Green PCR master mix PA-012 (SABiosciencesInc). The thermocycler parameters were 95°C for 10 minutes, followed by 40 cycles of 95°C for 15 seconds and 60°C for 1 minute. Relative changes in gene expression were calculated via SuperArray PCR Array Data Analysis Software using the cycle threshold (Ct) method with normalization of the raw data to several housekeeping genes. The expression data are presented as actual change multiples. We also performed QPCR using prevalidated primer sets (SuperArray Bioscience) for mRNAs encoding Postsynaptic Density Protein 95 (PSD95; PPH01848A), Spinophilin (SPN; PPM34114A), Synaptophysin (SYP; PPM03241A), N-Methyl-D-Aspartate Receptor Subunit NR1 (NMDAR1;PPH01823F), AChE (PPM35356A), and ACTB (PPM02945B). We used ACTB as an internal control for normalization. Reactions were run on a CFX96 using Real-Time SYBR Green PCR master mix PA-012 (SuperArray Bioscience). The thermocycler parameters were 95°C for 10 minutes, followed by 40 cycles of 95°C for 15 seconds and 72°C for 30 seconds. Relative changes in gene expression were calculated using the Ct (cycle threshold) method. The expression data are presented as actual change multiples32 (Livak and Schmittgen 2001).

We chose PSD95, NMDAR1, SPN and SYP genes to determine the effect of CPF on dendritic spine density, because both genes are the main regulators of dendritic spine plasticity[33,35].

Statistical analysis

At least three replicates for each experimental condition were performed, and the presented results were representative of these replicates. Data are represented as means ± standard deviation (SD). Comparisons between experimental and control groups were performed by Student's *t* test and ANOVA analyses followed by the Tukey post-hoc test. Statistical difference was accepted when p≤ 0.05. Statistical analysis of data was carried out by computer using GraphPad software.

Results

Effect of CPF on SN56 cell viability

We used the LDH assay to evaluate cell survival after 24 h and 14 days exposure to CPF at increasing concentrations. LDH is released from cells as a result of loss of plasma membrane integrity and it is indicative of necrotic cell death mechanism. An increased LDH release to the medium was observed in a dose dependent way after 24 h and long-term CPF exposure from 50 μM and 20 μM concentrations respectively compared with vehicle-treated cells (control negative) (**Figure 1**). Moreover, after CPF treatment of SN56 AChE silenced cells amelioration in LDH release was also observed (**Figure 1**). There was no significant difference between data of vehicle-treated cells and control cells.

AChE gene knockdown

To investigate the protection afforded by the knockdown of the AChE during cell death, we introduced siRNA oligonucleotides into SN56 cells by transfection directed against AChE. Transfection of cells with control siRNA showed no effect on AChE gene expression or cell viability, but the AChE siRNA caused large reductions in AChE gene expression (**Figure 2**). Cultures transfected with control siRNA compared with culture transfected against AChE, showed no effect in cell viability by LDH assays (**Figure 2**).

Effect of CPF on dendritic spine density

We observed that CPF induces acute (from 1 μM) and long-term (from 0.1 μM), concentration-dependent, reduction in the number of dendritic spine-like processes per length of neurite compared with vehicle treated on SN56 cultured neurons (**Figure 3**). There was no effect of treatment on mean soma size or the number of neurites per neuron (Data not shown).

Real-time PCR analysis

After incubation for 24 h and 14 days with 0.01 μM and 30 μM concentrations of CPF in SN56 cells, necrotic and apoptotic gene expression profile of CPF was analyzed with our Real-time PCR arrays. Moreover, the CPF effect on AChE and the main regulator dendritic spines synaptic plasticity gene expression in AChE silenced Cells and wild type respectively were analyzed. The gene expression profile of CPF was significantly different from normal control. The results show that after 24 h and 14 days exposure at 0.01 μM concentration of CPF only the expression of TNF, TNFRSF1A, TNFRSF10A, TNFRSF11B proapoptotic

Figure 1: CPF (0.01 to 70 µM) effect on cell viability of SN56 wild type or AChE silenced was determined by LDH release assays. Results are expressed as percentages of LDH release after subtracting the control values. Data represents the mean ± SD of three separate experiments from cells of different cultures, each one performed in triplicate. ***p<0.001 compared to control. &&&p≤0.001 compared to CPF treatment.
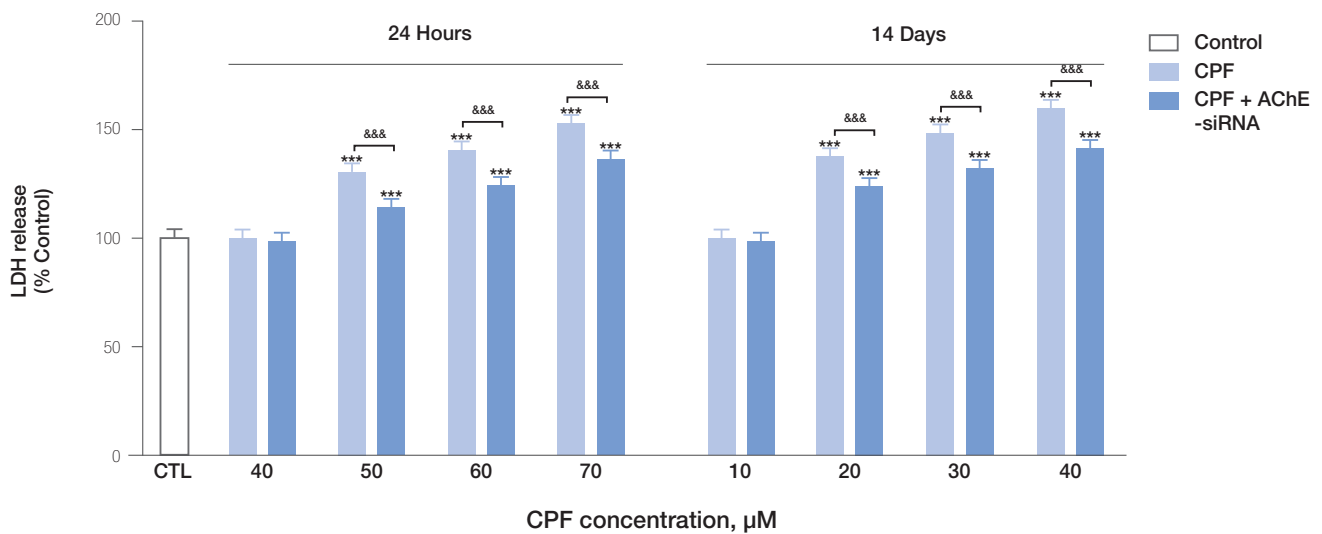

genes, TRAF2, BICR2 and BIRC3 antiapoptotic genes and MAG, S100A7A and KCN1P1 genes related with necrosis process was induced (**Table I** and **II**). Moreover, after 24 h exposure at 30 µM concentration of CPF 27 genes were up-regulated and 5 genes were down-regulated with a fold change higher and lower than 1.5 respectively for CPF compared with normal control (**Table I**). In addition, after and 14 days exposure at 30 µM concentration of CPF 43 genes were up-regulated and 7 genes were down-regulated with a fold change higher and lower than 1.5 respectively for CPF compared with normal control (**Table II**). Finally, we observed that after acute (from 0.01 µM) and long term (from 0.01 µM) CPF exposure, a concentration-dependent reduction in PSD95 and SYP gene expression (**Figure 4A** and **4B**), but we only observed a concentration-dependent gene expression reduction of SPN and NMDANR1 after acute exposure from 1 µM CPF concentration and after long-term exposure from 0.1 µM CPF concentrations (**Figure 4C** and **4D**).

Discussion

In the present work we show that CPF induces acute (from 50µM) and long-term (from 20 µM), concentration-dependent, necrotic cell death on septal SN56 cholinergic basal forebrain neurons. These results are supported by previous works which showed that CPF induced neuronal cell death through necrosis process after CPF acute and long-term exposure[12,13]. Previously, we found that CPF induces acute (from 30µM) and long-term (from 1 µM), concentration-dependent, cell death on septal SN56 cholinergic basal forebrain neurons, showing that apoptotic process is involved in this effect mediated partially by AChE variants overexpression[11]. Moreover, we show that the increase in LDH release was mediated partially by AChE overexpression. In this regard, Del Pino et

Figure 2: Downregulation of AChE in SN56 cells and its impact on cell viability and gene expression was determined. Control: SN56 cells transfected without siRNA. Negative (Neg.) control: SN56 cells transfected with scrambled siRNA. AChE-siRNA: transfected with siRNA against AChE. (A) LDH assays shows that AChE downregulation did not significantly induce cell damage after 48 h. (B) AChE downregulation could be detected by RT-PCR analysis 48 h after transfection. Values are given as mean ± SD of three separate experiments from cells of different cultures, each one performed in triplicate. ***p<0.001 compared to control.
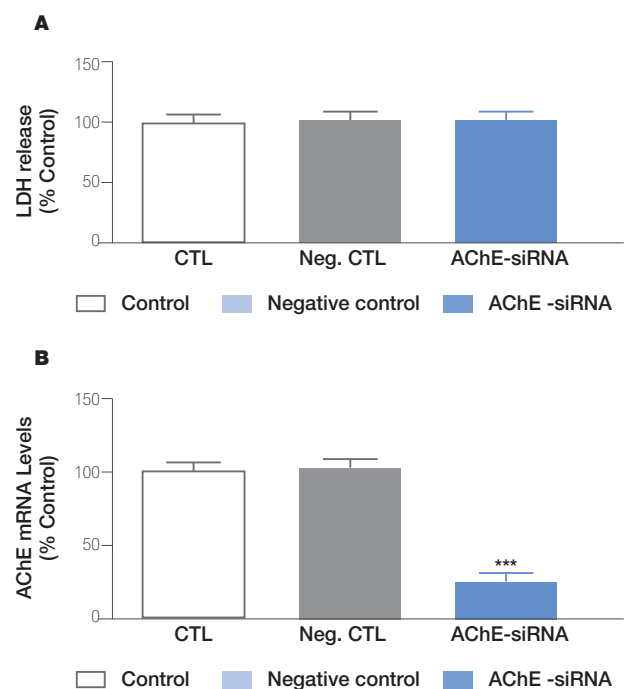
al[14] reported that AChE-R and AChE-S overexpression induces at low concentrations apoptosis and necrosis at higher concentrations in basal forebrain cholinergic neurons, supporting our results. Basal forebrain cholinergic neurons loss has been related with cognitive deficits[36-40]. In fact, the severity of memory deficit is strongly corre-

Figure 3: Effects of different CPF concentrations for 24 h or 14 days on dendritic spine density were determined in neurite SN56 cells. Dendritic spine density is indicated as % of control (CTL, white column). Data represents the mean ± SD of three independent experiments in triplicate. ***p<0.001 compared to control.
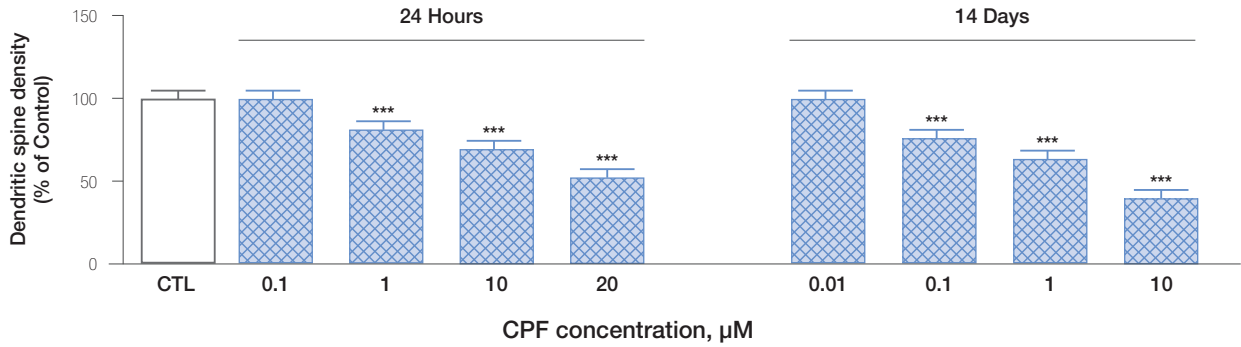

Figure 4: Shows results from real-time PCR arrays targeting (A) PSD95, (B) SYP, (B) SPN and (D) NMDAR1 genes after 24 h and 14 days CPF treatment. SD95, SYP, SPN and NMDAR1 gene expression was compared with controls. Each bar represents mean ± SD of 6 samples. Levels were measured using QPCR. ACTB was used as an internal control. ***p<0.001, significantly different from controls.
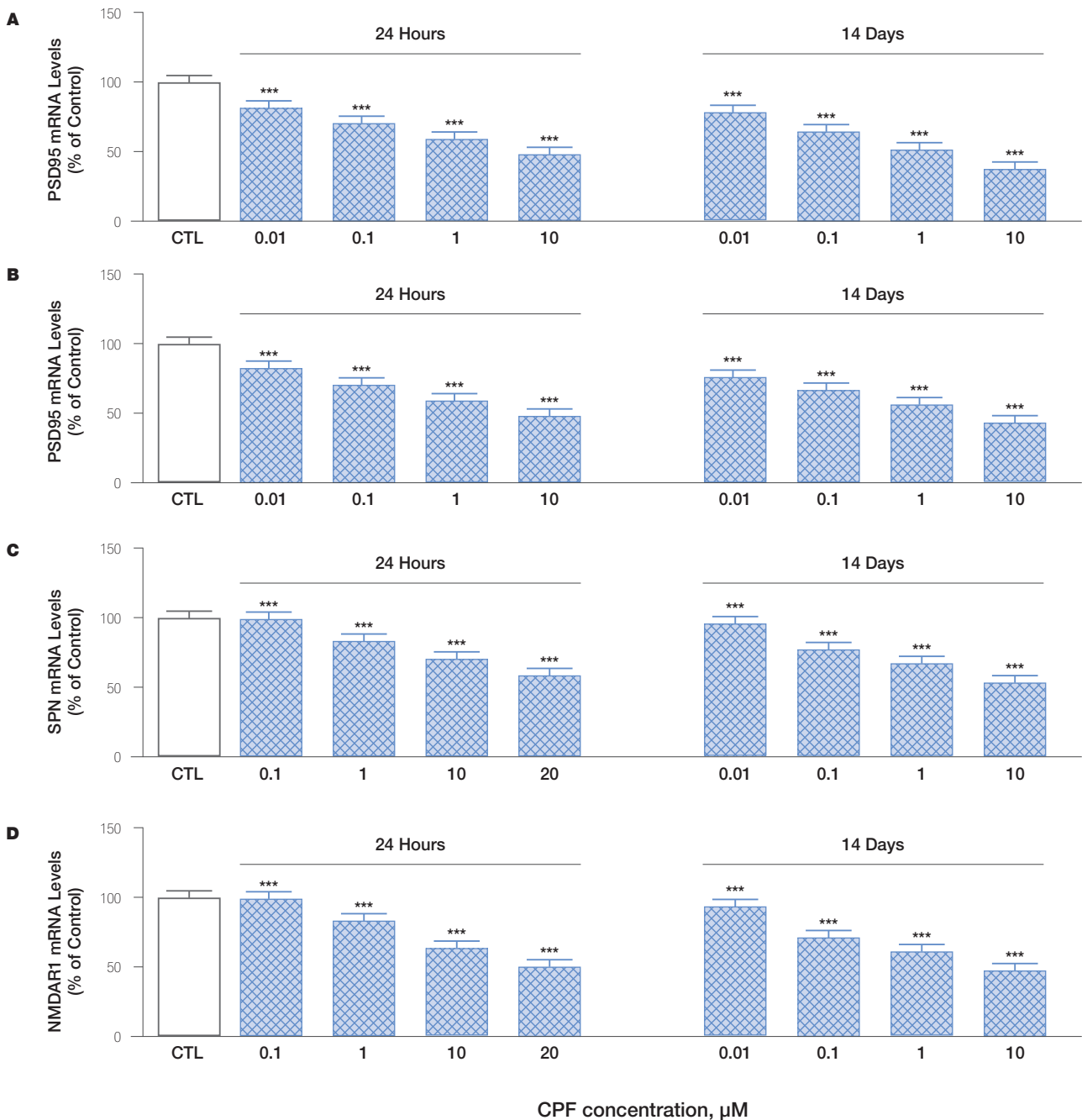
Table I: Fold-change of cell death related genes after 24 h CPF treatment. Values on red or blue mean a fold change upper or downer than 2

Gene Symbol	GenBank Accession No.	Fold Change 0.01μM	Fold Change 30μM	Gene Symbol	GenBank Accession No.	Fold Change 0.01μM	Fold Change 30μM
ABL1	NM_005157	1,11[b]	1,23[a]	FOXI1	NM_012188	1,12[a]	0,07
AKT1	NM_005163	1,02	1,05	GAA	NM_000152	1,09	1,19[a]
APAF1	NM_001160	1,15[b]	2,52[a]	GADD45A	NM_001924	1,11[a]	2,24[a]
APP	NM_000484	1,16[a]	1,41[a]	GALNT5	NM_014568	1,03	1.05
ATG12	NM_004707	1,17[a]	1,13[a]	GRB2	NM_002086	1,06	1,09
ATG16L1	NM_017974	1,21[a]	1,16[a]	HSPBAP1	NM_024610	1,05	1,13[a]
ATG3	NM_022488	1,04	1,11[a]	HTT	NM_002111	1,06	1,23[a]
ATG5	NM_004849	1,01	1,21[a]	IFNG	NM_000619	1,07	1,08
ATG7	NM_006395	1,04	1,04	IGF1	NM_000618	1,01	1,14[a]
ATP6V1G2	NM_130463	1,02	1,02	IGF1R	NM_000875	1,02	1,09
BAX	NM_004324	1,05	2,54[a]	INS	NM_000207	1,07	1,11[b]
BCL2	NM_000633	1,10[b]	1,15[a]	IRGM	NM_001145805	1,13[b]	1,28[a]
BCL2A1	NM_004049	1,02	1,04	JPH3	NM_020655	1,09	1,06
BCL2L1	NM_138578	1,13[a]	2,23[a]	KCNIP1	NM_014592	2,51[a]	3,21[a]
BCL2L11	NM_006538	1,01	2,32[a]	MAG	NM_002361	2,12[a]	2,69[a]
BECN1	NM_003766	1,03	1,06	MAP1LC3A	NM_181509	1,08	2,35[a]
BIRC2	NM_001166	1,72[a]	-1,43[a]	MAPK8	NM_002750	1,07	1,17[b]
BIRC3	NM_001165	1,69[a]	-1,59[a]	MCL1	NM_021960	1,14[a]	1,27[a]
BMF	NM_033503	1,06	1,06	NFKB1	NM_003998	1,02	1,06
C1orf159	NM_017891	1,13[a]	1,16[a]	NOL3	NM_003946	1,05	1,04
CASP1	NM_033292	1,05	2,21[a]	OR10J3	NM_001004467	1,01	1,07
CASP2	NM_032982	1,01	1,09	PARP1	NM_001618	1,11[a]	1,03
CASP3	NM_004346	1,05	1,57[a]	PARP2	NM_005484	1,06	1,01
CASP6	NM_032992	1,06	1,25[a]	PIK3C3	NM_002647	1.07	1.05
CASP7	NM_001227	1,02	2,31[a]	PVR	NM_006505	1,06	1,10[a]
CASP9	NM_001229	1,01	1,69[a]	RAB25	NM_020387	1,03	1,02
CCDC103	NM_213607	1,07	1,05	RPS6KB1	NM_003161	1,27[a]	1,31[a]
CD40	NM_001250	1,08	3,31[a]	S100A7A	NM_176823	2,17[a]	2,47[a]
CD40LG	NM_000074	1,06	3,56[a]	SNCA	NM_000345	1,06	1,25[a]
CFLAR	NM_003879	1,21[a]	1,11[a]	SPATA2	NM_006038	1,12[a]	2,41[a]
COMMD4	NM_017828	1,02	1,02	SQSTM1	NM_003900	1,17[a]	1,12[a]
CTSB	NM_001908	1,13[a]	1,05	SYCP2	NM_014258	1,03	1,66[a]
CTSS	NM_004079	1,08	1,04	TMEM57	NM_018202	1,11[a]	1,15[a]
CYLD	NM_015247	1,12[a]	1,08	TNF	NM_000594	1,53[a]	1,69[a]
DEFB1	NM_005218	1,01	1,01	TNFRSF10A	NM_003844	1,61[a]	1,78[a]
DENND4A	NM_005848	1,03	1,33[a]	TNFRSF11B	NM_002546	2,01[b]	2,37[b]
DFFA	NM_004401	1,05	1,09	TNFRSF1A	NM_001065	1,75[a]	1,91[a]
DPYSL4	NM_006426	1,01	1,05	TP53	NM_000546	1,10	1,67[a]
EIF5B	NM_015904	1,03	1,33[b]	TRAF2	NM_021138	2,22[a]	2,72[a]
ESR1	NM_000125	1,04	1,07	TXNL4B	NM_017853	1,01	1,69[a]
FAS	NM_000043	1,02	2,31[a]	ULK1	NM_003565	1,02	1,04
FASLG	NM_000639	1,06	2,13[a]	XIAP	NM_001167	1,05	1,01

[a] $p < 0.001$ compared to the control.   [b] $p < 0.05$ compared to the control.

lated with the degree of cholinergic cell loss[9]. Thus, the observed effects on cholinergic basal forebrain neurons may be, in part, responsible for the learning deficits and neurodegenerative disease symptoms like observed after acute and long-term exposure to CPF.

Moreover, after acute (from 0.01 μM) and long-term (from 0.01 μM) CPF exposure we only observed an induction in the gene expression of TNF, TNFRSF1A, TNFRSF10A, TNFRSF11B proapoptotic genes, TRAF2, BICR2 and BIRC3 antiapoptotic genes and MAG, S100A7A and KCN1P1 genes related with necrosis process. Apoptosis is triggered through the extrinsic pathway when extracellular stimuli and the cytokines CD40L, FASLG, TNFSF10 and TNF-α inducing cytokine receptors, including FAS receptor and tumor necrosis factor super family receptors (TNFRs) like TNFRSF1A, TNFRSF1B, TNFRSF10B and CD40, are activated[41,42]. Inhibitors of apoptosis

BIRC3 and BIRC2, through TRAF2, can prevent its activation[43]. According to this, CPF could activate cell death through extrinsic partway, but was blocked by activation of apoptosis inhibitors. Otherwise, MAG and S100A7A genes have been related with necrosis induction[44] and KChIP1 expression has been reported to play a protective role against cell death and its downregulation leads to the induction of necrotic cell death[45]. Therefore, KChIP1 overexpression after CPF exposure could be a protective mechanism against cell injury produced by CPF.

In addition, after acute (30 μM) CPF exposure the gene expression resultant showed a fold change greater or lower than 1.5 in the expression of the 29 genes related to apoptosis and necrosis for CPF treatment. Our research showed that CPF increased the expression of CD40, CD40LG, FAS, FASLG, TNF, TNFRSF10A, TNFRSF1A, TNFRSF11B, which likely leaded to induce

Table II: Fold-change of cell death related genes after 14 days CPF treatment. Values on red or blue mean a fold change upper or downer than 2

Gene Symbol	GenBank Accession No.	Fold Change		Gene Symbol	GenBank Accession No.	Fold Change	
		0.01μM	30μM			0.01μM	30μM
ABL1	NM_005157	1,15[b]	1,32[a]	FOXI1	NM_012188	1,15[a]	2,14[a]
AKT1	NM_005163	1,07	1,08	GAA	NM_000152	1,04	1,32[a]
APAF1	NM_001160	1,18[a]	2,56[a]	GADD45A	NM_001924	1,14[a]	2,22[a]
APP	NM_000484	1,19[a]	1,31[a]	GALNT5	NM_014568	1,06	-1,64
ATG12	NM_004707	1,18[a]	1,24[a]	GRB2	NM_002086	1,04	2,51[a]
ATG16L1	NM_017974	1,19[a]	1,33[a]	HSPBAP1	NM_024610	1,07	1,69[a]
ATG3	NM_022488	1,07	1,19[a]	HTT	NM_002111	1,03	1,13[a]
ATG5	NM_004849	1,04	1,62[a]	IFNG	NM_000619	1,05	1,02
ATG7	NM_006395	1,03	1,84[a]	IGF1	NM_000618	1,06	1,16[a]
ATP6V1G2	NM_130463	1,01	1,59[a]	IGF1R	NM_000875	1,03	1,05
BAX	NM_004324	1,09	2,69[a]	INS	NM_000207	1,06	1,11[a]
BCL2	NM_000633	1,13[a]	1,19[a]	IRGM	NM_001145805	1,10[b]	1,29[a]
BCL2A1	NM_004049	1,05	1,08	JPH3	NM_020655	1,05	2,38[a]
BCL2L1	NM_138578	1,08	2,27[a]	KCNIP1	NM_014592	2,62[a]	-3,67[a]
BCL2L11	NM_006538	1,07	2,34[a]	MAG	NM_002361	2,25[a]	-3,42[a]
BECN1	NM_003766	1,07	1,09	MAP1LC3A	NM_181509	1,04	2,42[a]
BIRC2	NM_001166	1,86[a]	-1,62[a]	MAPK8	NM_002750	1,02	1,21[b]
BIRC3	NM_001165	1,82[a]	-1,53[a]	MCL1	NM_021960	1,10[b]	1,29[a]
BMF	NM_033503	1,09	2,95[a]	NFKB1	NM_003998	1,03	1,07
C1orf159	NM_017891	1,12[a]	3,76[a]	NOL3	NM_003946	1,06	1,02
CASP1	NM_033292	1,02	2,19[a]	OR10J3	NM_001004467	1,05	-3,67[a]
CASP2	NM_032982	1,03	1,15[a]	PARP1	NM_001618	1,13[a]	1,74[a]
CASP3	NM_004346	1,07	1,72[a]	PARP2	NM_005484	1,02	1,81[a]
CASP6	NM_032992	1,04	1,23[a]	PIK3C3	NM_002647	1,05	2,28[a]
CASP7	NM_001227	1,03	2,22[a]	PVR	NM_006505	1,08	1,49[a]
CASP9	NM_001229	1,06	1,68[a]	RAB25	NM_020387	1,04	1,04
CCDC103	NM_213607	1,13[a]	2,31[a]	RPS6KB1	NM_003161	1,15[a]	1,19[a]
CD40	NM_001250	1,08	4,48[a]	S100A7A	NM_176823	2,28[a]	-2,73[a]
CD40LG	NM_000074	1,06	3,16[a]	SNCA	NM_000345	1,03	1,29[a]
CFLAR	NM_003879	1,21[a]	1,27[a]	SPATA2	NM_006038	1,10[b]	2,36[a]
COMMD4	NM_017828	1,02	2,12[a]	SQSTM1	NM_003900	1,12[a]	1,19[a]
CTSB	NM_001908	1,13[a]	2,52[a]	SYCP2	NM_014258	1,05	1,67[a]
CTSS	NM_004079	1,05	2,26	TMEM57	NM_018202	1,13[a]	1,24[a]
CYLD	NM_015247	1,10[b]	2,22[a]	TNF	NM_000594	1,59[a]	1,66[a]
DEFB1	NM_005218	1,04	1,93[a]	TNFRSF10A	NM_003844	1,72[a]	1,79[a]
DENND4A	NM_005848	1,01	1,35[b]	TNFRSF11B	NM_002546	2,14[b]	2,26[b]
DFFA	NM_004401	1,03	1,03	TNFRSF1A	NM_001065	1,83[a]	1,91[a]
DPYSL4	NM_006426	1,06	2,81	TP53	NM_000546	1,18	1,85[a]
EIF5B	NM_015904	1,01	1,33[b]	TRAF2	NM_021138	2,31[a]	3,14[a]
ESR1	NM_000125	1,02	1,01	TXNL4B	NM_017853	1,11	1,69[a]
FAS	NM_000043	1,05	2,36[a]	ULK1	NM_003565	1,09	1,02
FASLG	NM_000639	1,03	2,46[a]	XIAP	NM_001167	1,06	1,04

[a] $p < 0.001$ compared to the control.   [b] $p < 0.05$ compared to the control.

apoptosis through extrinsic pathway. CPF increased also the expression of TRAF2 and decreased BIRC3 and BIRC2 antiapoptotic genes allowing caspases activation which expression was increased. Besides, CPF induced GADD45A, and TP53 genes expression. The P53-GADD45A pathway has been shown to primarily play a role in the control of G2-M arrest following certain DNA-damaging agents[46,47], thus their induction could lead to cell arrest. Moreover, CPF increased the expression of BAX and BCL2L11 proapoptotic genes and BCL2L1 antiapoptoptic gene[48], further decrease the ratio BCL2/BAX which regulated the induction of apoptosis[49] leading to apoptosis. Finally, CPF increased the expression of CASP1, CASP3, CASP7, CASP9 which executed apoptosis. Besides, CPF increased the expression of KCN1P1, MAG and S100A7A genes related to necrosis as happened at lower concentrations indicating that necrosis is prevented.

After long-term CPF exposure (30 μM), besides the effect on the same genes commented after acute exposure, CPF increased the expression of ATP6VG2, BMF, CLORF159, CCDC103, COMMD4, CTSB, STSS, CYLD, DEFB1, DPYSL4, FOXIL1, GRB2, HSPBAP1, JPH3, PARP1, PARP2, PIK3C3, PVR, TXNL4B and decreased the expression of GALNTL5, OR10J3, KCN1P1, MAG and S100A7A genes related to necrosis according with the research of Hitomi et al[44]. Our study indicates that CPF exerts its cell death effects by involving apoptosis and necrosis pathways.

Otherwise, we observed that CPF induces acute (from 1 μM) and long-term (from 0.1 μM), concentration-dependent, reduction in the number of dendritic spine density on septal SN56 cholinergic basal forebrain neurons. In this regard, CPF has been reported to induce an alteration in the dendritic spines density in the prefrontal cortex and hip-

pocampus after acute and repeated exposure to subclinical doses respectively[18,19], supporting our results. Dendritic spines loss has been reported in neurodegenerative disorders as AD, affecting mostly selective neuronal networks of critical importance for memory and cognition, such as the basal forebrain cholinergic system, the medial temporal regions, the hippocampus and many neocortical association areas[15] inducing cognitive disorders[16,17]. Moreover, cognitive disorders have been reported to be produced from subclinical doses and from lower doses from which basal forebrain cholinergic cell loss has been reported[20], as happens with dendritic spines alteration, suggesting that both processes are implicated in cognitive disorders induction, at low doses only through dendritic spine alteration and at higher doses through both mechanisms.

In addition, we observed that after acute (from 0.01 μM) and long term (from 0.01 μM) CPF exposure, a concentration-dependent downregulation in PSD95 and SYP gene expression was produced. It has been suggested that SYP plays a role in formation and stabilization of synapses[50], regulating dendritic spine density and shape[51,52]. Moreover, PSD95 was described to play a role in determining the size and the strength of synapses[53,54], formation of synapse assemblies[54] and spine-maturation[55,56]. Therefore, both genes alteration could be implicated in the effects observed on dendritic spines. Our results show that PSD95 and SYP gene expression is altered below the concentration from which dendritic spine density disruption is evident, which indicates that the harmful effects of CPF exposure on dendritic spines could be started and detected before they would be manifest and these genes could be used as biomarker of this effect. Moreover, PSD95 and SYP are both involved in dendritic spine morphology regulation and their alteration by CPF exposure may be involved with a disruption of dendrite spine shape, contributing to the cognitive disorders observed. Otherwise, we only observed a concentration-dependent SPN and NMDANR1 gene expression downregulation after acute exposure from 1 μM CPF concentration and after long-term exposure from 0.1 μM CPF concentrations as seen with dendritic spines density reduction, suggesting both genes are directly correlated with this effect. In this regard, SPN, a key cytoskeletal protein in the formation and maintenance of dendritic spines, has been reported to modulate dendritic morphology and number[33] and an increase in dendritic spine density has been correlated with an increase in the spinophilin expression[34]. In addition, N-methyl-D-aspartate (NMDA) receptor, is also involved in synaptic plasticity as well as learning and memory processes regulation[57] and the N-methyl-D-aspartate receptor antagonists reduce dendritic spine density and neurite growth[35]. Future studies are needed to determine the implication of these genes in dendritic spine shape and density disruption mechanisms.

According to all exposed above, CPF induced changes on cell death and dendritic spines plasticity pathways were detected at doses below those required to induce manifest

apoptotic and necrotic cell death and alter dendritic spines plasticity. These results support the suggestion that gene expression changes could potentially be more sensitive measures of effects at early stages and at lower doses than many typical toxicological measures[58] and that altered toxicogenomic profiles contributing to toxicologically-relevant pathways provide useful tools for more precise determination of toxicological mechanisms as compared to traditional toxicological endpoints and for reducing uncertainty in establishing lowest observed adverse effect level (LOAEL), no observed adverse effect level (NOAEL), or benchmark dose (BMD)[59-62]. Therefore, the toxicogenomic profile analysis could offer means to improve human health risk assessment generally based on standard toxicity test results. Previously, this approach has been employed in different studies as the published by Lobenhofer et al[60] that examines *in vitro* transcriptional responses to very low concentrations of estrogen, confirming that estrogen concentrations below those which are physiologically relevant did not induce a measurable transcriptional response. That concentration threshold was referred to as the No Observable Transcriptional Effect Level (NOTEL). In our study, it was shown that the CPF Lowest Observed Adverse Transcriptional Expression Levels (LOATEL) for 12 responding genes was at least 100-fold lower than the NOAEL that was based on observable inhibition of erythrocyte acetylcholinesterase activity in humans[30]. Therefore, lower doses would be needed in order to observe no transcriptional effects. Examination of data from the group of 12 responding genes leads us to propose 0.003-0.004 mg/kg/day as LOATEL for CPF. The present study did not, therefore, establish a No Observed Adverse Transcriptional Effect Level (NOATEL) for CPF. These subclinical transcriptional changes may be employed as predictors of adverse effects from toxic compounds exposure and thereby used to improve risk assessment and safety evaluation. Further studies are required to confirm this LOATEL.

Conclusion

Taking all together, it can be concluded that after acute and long-term exposure, CPF induces at low concentration a dendritic spine density reduction and at higher concentrations induces cell death on cholinergic neurons from basal forebrain through apoptotic and necrotic mechanisms, depending on the exposure concentration mediated in part though AChE variants overexpression and these effects were initiated at lower concentration that which they are manifest, as indicated by transcriptional alterations of key genes. Our results, particularly those for CPF treatment, suggest that toxicogenomic profiles provide a sensitive tool for identifying and characterizing thresholds of toxicity for potentially toxic compounds based upon a transcriptome-level of insight into their mechanisms. These effects could explain cognitive alterations and neurodegenerative diseases induced by CPF. In this regard, all the mechanisms that we reported to induce cholinergic cell loss in

basal forebrain have been described to be involved with the induction of cognitive disorders, which supports this hypothesis. Future studies should be developed to determine the other mechanisms implicated in these effects observed on cholinergic neurons. These results are of interest, since they provide new information on the mechanisms that mediate dendritic spine density alteration and cell death induce by CPF, and because they lead to a better understanding of some effects related to CPF toxicity and highlight the need for a new NOAEL and LOAEL and a new risk assessment of this pesticide.

Conflicts of interest statement

There are no conflicts of interest to declare.

Acknowledgments

References

1. Richardson JR, and Chambers JE. Effects of repeated oral postnatal exposure to chlorpyrifos on cholinergic neurochemistry in developing rats. Toxicol Sci. 2005; 84 (2): 352-9.

2. Hernandez CM, Beck WD, Naughton SX, Poddar I, Adam BL, Yanasak N, Middleton, C, and Terry AV Jr. Repeated exposure to chlorpyrifos leads to prolonged impairments of axonal transport in the living rodent brain. Neurotoxicology. 2015; 47: 17-26.

3. Rohlman DS, Anger WK, and Lein PJ. Correlating neurobehavioral performance with biomarkers of organophosphorous pesticide exposure. Neurotoxicology.2001; 32(2): 268-76.

4. Lopez-Granero C, Cardona D, Gimenez E, Lozano R, Barril J, Sanchez-Santed F, and Canadas F. Chronic dietary exposure to chlorpyrifos causes behavioral impairments, low activity of brain membrane-bound acetylcholinesterase, and increased brain acetylcholinesterase-R mRNA. Toxicology. 2013; 308: 41-9.

5. Middlemore-Risher ML, Buccafusco JJ, and Terry, AV Jr. Repeated exposures to low-level chlorpyrifos results in impairments in sustained attention and increased impulsivity in rats. NeurotoxicolTeratology. 2010; 32(4): 415-24.

6. Moser VC, Phillips PM, McDaniel KL, Marshall RS, Hunter DL, and Padilla S. Neurobehavioral effects of chronic dietary and repeated high-level spike exposure to chlorpyrifos in rats. ToxicolSci. 2005; 86 (2): 375-86.

7. Samsam TE, Hunter DL, and Bushnell PJ. Effects of chronic dietary and repeated acute exposure to chlorpyrifos on learning and sustained attention in rats. Toxicol Sci. 2005; 87(2): 460-8.

8. Scheiderer CL, McCutchen E, Thacker EE, Kolasa K, Ward MK, Parsons D, Harrell L. E, Dobrunz LE, and McMahon LL. Sympathetic sprouting drives hippocampal cholinergic reinnervation that prevents loss of a muscarinic receptor-dependent long-term depression at CA3-CA1 synapses. J Neurosci. 2006; 26(14): 3745-56.

9. Bierer LM, Haroutunian V, Gabriel S, Knott PJ, Carlin LS, Purohit DP, Perl DP, Schmeidler J, Kanof P, and Davis KL. Neurochemical correlates of dementia severity in Alzheimer's disease: relative importance of the cholinergic deficits. J Neurochem. 1995; 64(2): 749-60.

10. Andersson H, Petersson-Grawe K, Lindqvist E, Luthman J, Oskarsson A, and Olson L. Low-level cadmium exposure of lactating rats causes alterations in brain serotonin levels in the offspring. NeurotoxicolTeratol. 1997; 19: 105-15.

11. Del Pino J, Moyano P, Anadon MJ, Garcia JM, Diaz MJ, Garcia J, and Frejo MT. Acute and long-term exposure to chlorpyrifos induces cell death of basal forebrain cholinergic neurons through AChE variants alteration. Toxicology. 2015; 336: 1-9.

12. Kammon AM, Brar RS, Sodhi S, Banga HS, and Sandhu HS. Neuropathological Studies of Chickens Following Exposure to Chlorpyrifos. Toxicology International. 2010; 17, 78-81.

13. Nasr HM, El-Demerdash FM, and El-Nagar WA. Neuro and renal toxicity induced by chlorpyrifos and abamectin in rats: Toxicity of insecticide mixture. Environ Sci Pollut Res Int. 2016; 23: 1852-9.

14. Del Pino J, Zeballos G, Anadon MJ, Capo MA, Diaz MJ, Garcia J, and Frejo MT. Higher sensitivity to cadmium induced cell death of basal forebrain cholinergic neurons: a cholinesterase dependent mechanism. Toxicology. 2014; 325: 151-9.

15. Baloyannis SJ. Brain capillaries in Alzheimer's disease. Hell J Nucl Med. 2015; 1: 152.

16. Hains AB, Yabe Y, and Arnsten AFT. Chronic Stimulation of Alpha-2A-Adrenoceptors With Guanfacine Protects Rodent Prefrontal Cortex Dendritic Spines and Cognition From the Effects of Chronic Stress. Neurobiology of stress. 2015; 2: 1-9.

17. Mandolesi L, De Bartolo P, Foti F, Gelfo F, Federico F, Leggio MG, and Petrosini L. Environmental enrichment provides a cognitive reserve to be spent in the case of brain lesion. J Alzheimers Dis. 2008; 15: 11-28.

18. Oostingh GJ, Wichmann G, Schmittner M, Lehmann I, and Duschl A. The cytotoxic effects of the organophosphates chlorpyrifos and diazinon differ from their immunomodulating effects. J Immunotoxicol. 2009; 6: 136-45.

19. Speed HE, Blaiss CA, Kim A, Haws ME, Melvin NR, Jennings M, Eisch AJ, and Powell CM. Delayed reduction of hippocampal synaptic transmission and spines following exposure to repeated subclinical doses of organophosphorus pesticide in adult mice. Toxicol Sci. 2012; 125: 196-208.

20. Terry AV Jr, Stone JD, Buccafusco JJ, Sickles DW, Sood A, and Prendergast MA. Repeated exposures to subthreshold doses of chlorpyrifos in rats: hippocampal damage, impaired axonal transport, and deficits in spatial learning. J Pharmacol Exp Ther. 2003; 305(1): 375-84.

21. Hammond DN, Lee, HJ, Tonsgard JH, and Wainer BH. Development and characterization of clonal cell lines derived from septal cholinergic neurons. Brain Res. 1990; 512 (2): 190-200.

22. Hudgens ED. Ji L, Carpenter CD, and Petersen SL. The gad2 promoter is a transcriptional target of estrogen receptor (ER) alpha and ER beta: a unifying hypothesis to explain diverse effects of estradiol. J Neurosci. 2009; 29(27): 8790-7.

23. Bielarczyk H, Jankowska A, Madziar B, Matecki A, Michno A, andSzutowicz A.Differential toxicity of nitric oxide, aluminum, and amyloid-β-peptide in SN56 cholinergic cells from mouse septum. Neurochem Int. 2003; 42: 323-31.

24. Szutowicz A, Bielarczyk H, Gul S, Ronowska A, Pawełczyk T, and Jankowska-Kulawy A. Phenotype-dependent susceptibility of cholinergic neuroblastoma cells to neurotoxic inputs. Met Brain Dis. 2006; 21: 149-61.

25. Crumpton TL, Seidler FJ, and Slotkin TA. Is oxidative stress involved in the developmental neurotoxicity of chlorpyrifos?. Brain Res Dev Brain Res. 2000; 121: 189-95.

26. Dam K, Garcia SJ, Seidler FJ, and Slotkin TA. Neonatal chlorpyrifos exposure alters synaptic development and neuronal activity in cholinergic and catecholaminergic pathways. Brain Res Dev Brain Res. 1999; 116 (1): 9-20.

27. Jett DA, and Navoa RV. In vitro and in vivo effects of chlorpyrifos on glutathione peroxidase and catalase in developing rat brain. Neurotoxicology. 2000; 21(1-2): 141-5.

28. Roy TS, Andrews JE, Seidler FJ, and Slotkin TA. Chlorpyrifos elicits mitotic abnormalities and apoptosis in neuroepithelium of cultured rat embryos. Teratology. 1998; 58(2), 62-8.

29. Nolan RJ, Rick DL, Freshour NL, and Saunders JH.Chlorpyrifos: pharmacokinetics in human volunteers. Toxicol Appl Pharmacol. 1984, 73 (1): 8-15.

30. JMPR. Pesticide Residues in Food–1999, Evaluations Part II: Toxicological WHO/PCS/00.4, FAO/WHO Pesticide Residues in Food, No 154, Joint Meeting of the FAO Panel of Experts on Pesticide Residues in Food and the Environment and the WHO Core Assessment Group on Pesticide Residues; World Health Organization: Geneva, Switzerland, 1999.

31. Wright CL, and McCarthy MM. Prostaglandin E2-induced masculinization of brain and behavior requires protein kinase A, AMPA/kainate, and metabotropic glutamate receptor signaling. J Neurosci. 2009; 29: 13274-82.

32. Livak KJ, and Schmittgen TD. Analysis of relative gene expression data using real-time quantitative PCR and the 2(-Delta DeltaC(T)) Method. Methods. 2001; 25(4): 402-8.

33. Feng J, Yan Z, Ferreira A, Tomizawa K, Liauw JA, Zhuo M, Allen PB, Ouimet CC, and Greengard P. Spinophilin regulates the formation and function of dendritic spines. Proc Natl Acad Sci USA. 2000; 97: 9287-92.

34. Hu J, Vidovic M, Chen MM, Lu QY, and Song, ZM. Activation of α2A adrenoceptors alters dendritic spine development and the expression of spinophilin in cultured cortical neurones. Brain Res. 2008; 1199: 37-45.

35. Zhang Q, Yu Y, and Huang XF. Olanzapine Prevents the PCP-induced Reduction in the Neurite Outgrowth of Prefrontal Cortical Neurons via NRG1. Sci Rep. 2016; 6: 19581.

36. Auld DS, Kornecook TJ, Bastianetto S, and Quirion R. Alzheimer's disease and the basal forebrain cholinergic system: relations to beta-amyloid peptides, cognition, and treatment strategies. Prog Neurobiol. 2002; 68: 209-45.

37. Kar S, Slowikowski SP, Westaway D, and Mount HT. Interactions between beta-amyloid and central cholinergic neurons: implications for Alzheimer's disease. J Psychiatry Neurosci. 2004; 29(6): 427-41.

38. Kesner RP, Adelstein TB, and Crutcher KA. Equivalent spatial location memory deficits in rats with medial septum or hippocampal formation lesions and patients with dementia of the Alzheimer's type. Brain Cogn. 1989; 9: 289-300.

39. Madziar B, Lopez-Coviella I, Zemelko V, and Berse B. Regulation of cholinergic gene expression by nerve growth factor depends on the phosphatidylinositol-3'-kinase pathway. J Neurochem. 2005; 92: 767-79.

40. Schliebs R. Basal forebrain cholinergic dysfunction in Alzheimer's disease--interrelationship with beta-amyloid, inflammation and neurotrophinsignaling. Neurochem Res. 2005; 30 (6-7): 895-908.

41. Davies CC, Mason J, Wakelam MJ, Young LS, and Eliopoulos AG. Inhibition of phosphatidylinositol 3-kinase- and ERK MAPK-regulated protein synthesis reveals the pro-apoptotic properties of CD40 ligation in carcinoma cells. J Biol Chem. 2004; 279 (2): 1010-9.

42. Thorburn A. Death receptor-induced cell killing. Cell Signal. 2004; 16: 139-44.

43. Mahul-Mellier AL, Pazarentzos E, Datler C, Iwasawa R, AbuAli G, Lin B, and Grimm S. De-ubiquitinating protease USP2a targets RIP1 and TRAF2 to mediate cell death by TNF. Cell Death Differ. 2012; 19 (5): 891-9.

44. Hitomi J, Christofferson DE, Ng A, Yao J, Degterev A, Xavier RJ, and Yuan J. Identification of a molecular signaling network that regulates a cellular necrotic cell death pathway. Cell. 2008; 135 (7): 1311-23.

45. Del Pino J, Frejo MT, Baselga MJ, Capo MA, Moyano P, Garcia JM, and Diaz MJ Neuroprotective or neurotoxic effects of 4-aminopyridine mediated by KChIP1 regulation through adjustment of Kv 4.3 potassium channels expression and GABA-mediated transmission in primary hippocampal cells. Toxicology. 2015; 333: 107-17.

46. Wang XW, Zhan Q, Coursen JD, Khan MA, Kontny HU, Yu L, Hollander MC, O'Connor PM, Fornace AJ Jr, and Harris CC. GADD45 induction of a G2/M cell cycle checkpoint. Proc Natl Acad Sci USA. 1999; 96 (7): 3706-11.

47. Jin S, Tong T, Fan W, Fan F, Antinore MJ, Zhu X, Mazzacurati L, Li X, Petrik KL, Rajasekaran B, Wu M, and Zhan Q.. GADD45-induced cell cycle G2-M arrest associates with altered subcellular distribution of cyclin B1 and is independent of p38 kinase activity. Oncogene. 2002; 21 (57): 8696-704.

48. Vogler M. BCL2A1: the underdog in the BCL2 family. Cell Death Differ. 2012; 19 (1): 67-74.

49. Oltvai ZN, Milliman CL, and Korsmeyer SJ. Bcl-2 heterodimerizes in vivo with a conserved homolog, Bax, that accelerates programmed cell death. Cell. 1993; 74 (4): 609-19.

50. Tarsa L, and Goda Y. Synaptophysin regulates activity-dependent synapse formation in cultured hippocampal neurons. Proc Natl Acad Sci USA. 2002; 99: 1012-6.

51. Glantz LA, Gilmore JH, Hamer RM, Lieberman JA, and Jarskog LF. Synaptophysin and postsynaptic density protein 95 in the human prefrontal cortex from mid-gestation into early adulthood. Neuroscience. 2007; 149: 582-91.

52. Li Q, Deng Z, Zhang Y, Zhou X, Nagerl UV, and Wong ST. A global spatial similarity optimization scheme to track large numbers of dendritic spines in time-lapse confocal microscopy. IEEE Trans Med Imaging. 2011; 30: 632-41.

53. Ehrlich I, and Malinow R. Postsynaptic density 95 controls AMPA receptor incorporation during long-term potentiation and experience-driven synaptic plasticity. J Neurosci. 2004; 24: 916-27.

54. Garner CC, Nash J, and Huganir RL. PDZ domains in synapse assembly and signalling. Trends Cell Biol. 2000; 10: 274-80.

55. El-Husseini AE, Schnell E, Chetkovich DM, Nicoll RA, and Bredt DS. PSD-95 involvement in maturation of excitatory synapses. Science. 2000; 290: 1364-8.

56. Nikonenko I, Boda B, Steen S, Knott G, Welker E, and Muller D. PSD-95 promotes synaptogenesis and multiinnervated spine formation through nitric oxide signaling. J Cell Biol. 2008; 183: 1115-27.

57. Kannangara TS, Bostrom CA, Ratzlaff A, Thompson L, Cater, RM, Gil-Mohapel J, and Christie, BR. Deletion of the NMDA receptor GluN2A subunit significantly decreases dendritic growth in maturing dentate granule neurons. PLoS One. 2014; 9: e103155.

58. Parfett C, Williams A, Zheng JL, and Zhou G (). Gene batteries and synexpression groups applied in a multivariate statistical approach to dose-response analysis of toxicogenomic data. Regul Toxicol Pharmacol. 2013; 67: 63-74.

59. Goldberg Z, Schwietert CW, Lehnert B, Stern R, and Nami I. Effects of low-dose ionizing radiation on gene expression in human skin biopsies. Int J Radiat Oncol Biol Phys. 2004; 58: 567-74.

60. Lobenhofer EK, Cui X, Bennett L, Cable PL, Merrick BA, Churchill GA, and Afshari CA. Exploration of low-dose estrogen effects: identification of No Observed Transcriptional Effect Level (NOTEL). Toxicol Pathol. 2004; 32: 482-92.

61. Schlecht C, Klammer H, Wuttke W, and Jarry H. A dose-response study on the estrogenic activity of benzophenone-2 on various endpoints in the serum, pituitary and uterus of female rats. Arch Toxicol. 2006; 80: 656-61.

62. Zheng JL, Parfett C, Williams A, Yagminas A, Zhou G, Douglas GR, and Yauk CL. Assessment of subclinical, toxicant-induced hepatic gene expression profiles after low-dose, short-term exposures in mice. Regul Toxicol Pharmacol. 2011; 60: 54-72.